

Reinvestigations of the $\text{Li}_2\text{O}-\text{Al}_2\text{O}_3$ system. Part I: LiAlO_2 and Li_3AlO_3

Piotr Tabero*, Artur Frąckowiak, Grażyna Dąbrowska

West Pomeranian University of Technology Szczecin, Faculty of Chemical Technology and Engineering, Department of Inorganic and Analytical Chemistry, Piastow Avenue 42, 71-065 Szczecin, Poland

*Corresponding author: e-mail: ptab@zut.edu.pl

Reinvestigations of the $\text{Li}_2\text{O}-\text{Al}_2\text{O}_3$ system focused on the synthesis and properties of LiAlO_2 and Li_3AlO_3 phases have been performed with the help of XRD and IR measuring techniques and Li_2CO_3 , $\text{LiOH}\cdot\text{H}_2\text{O}$, $\text{Al}_2\text{O}_3\text{-sl}$, $\alpha\text{-Al}_2\text{O}_3$, $\text{Al}(\text{NO}_3)_3\cdot 9\text{H}_2\text{O}$ and boehmite as reactants. Results of investigations have shown the formation of α -, β -, and γ - polymorphs of LiAlO_2 . It was found that only the use of $\text{LiOH}\cdot\text{H}_2\text{O}$ as a reactant yields to $\beta\text{-LiAlO}_2$ as a reaction product. On the other hand, it was proved that Li_3AlO_3 does not form in the $\text{Li}_2\text{O}-\text{Al}_2\text{O}_3$ system. A new method for the synthesis of $\alpha\text{-LiAlO}_2$ was developed, consisting in grinding the mixture of Li_2CO_3 and $\text{Al}(\text{NO}_3)_3\cdot 9\text{H}_2\text{O}$ and heating the obtained paste at the temperature range of 400–600 °C. The IR spectroscopy was used to characterize obtained phases.

Keywords: $\text{Li}_2\text{O}-\text{Al}_2\text{O}_3$ system, LiAlO_2 , Li_3AlO_3 , XRD, IR.

INTRODUCTION

Compounds containing lithium have been the subject of comprehensive research for many years due to many different industrial applications, including the production of glass and heat-resistant ceramics^{1–3}, luminescent ionizing radiation detectors^{4,5}, carbonate fuel cell components^{6–9}, carbon dioxide absorbents¹⁰ and solid electrolytes used for the production of lithium-ion batteries^{11,12}. Lithium aluminates are active catalysts for the hydrophosphinization of alkynes, alkenes and carbodiimides¹³. Lithium-based ceramics have been identified as the most important material for obtaining tritium in Test Modules (TBMs) of the International Thermonuclear Experimental Reactor Project, ITER^{14–18}.

The literature review has shown that 5 compounds are formed in the two-component system of $\text{Li}_2\text{O}-\text{Al}_2\text{O}_3$ oxides: Li_5AlO_4 , Li_3AlO_3 , $\text{LiAl}_2\text{O}_{3,5}$, LiAlO_2 and LiAl_5O_8 . Hatch¹⁹ suggests that limited or continuous solid solutions may form between LiAl_5O_8 and $\gamma\text{-Al}_2\text{O}_3$. So far, no phase diagram of the $\text{Li}_2\text{O}-\text{Al}_2\text{O}_3$ system has been developed in the entire concentration range of the components. There are two versions of the phase diagram of the system in the range of $\text{LiAlO}_2-\text{Al}_2\text{O}_3$ ^{20,21}, which show that one LiAl_5O_8 compound is formed. In none of these works, there was any information about the formation of the $\text{LiAl}_2\text{O}_{3,5}$ compound, mentioned by M. Kriens and co-authors²². There are three versions of the phase diagram of the $\text{Li}_2\text{O}-\text{Al}_2\text{O}_3$ system, developed based on thermodynamic data available in the literature^{23–25}.

Despite numerous studies on the $\text{Li}_2\text{O}-\text{Al}_2\text{O}_3$ system, there is still controversy about the number and type of phases formed in it, methods of their preparation and properties^{19–55}. Therefore, our work aimed to verify the literature data on the $\text{Li}_2\text{O}-\text{Al}_2\text{O}_3$ system. The first part of our investigations was focused on the LiAlO_2 and Li_3AlO_3 phases.

The LiAlO_2 compound has four polymorphic modifications^{26–46}: hexagonal α ^{26–29}, orthorhombic β ^{30,31}, tetragonal γ ³² and the $\delta\text{-LiAlO}_2$ formed at pressures above 9 GPa³³. High-pressure studies carried out by Lei et al.³⁴ showed that the monoclinic form of $\beta\text{-LiAlO}_2$ obtained by Cheng³⁵ under the pressure of 1.8 GPa is in fact the orthorhombic modification of $\beta\text{-LiAlO}_2$ and it can be obtained already at the pressure of 0.8 GPa and tem-

perature 623 K. On the other hand, the cubic form of LiAlO_2 described by Debray and Hardy³⁶ is in fact the tetragonal $\gamma\text{-LiAlO}_2$. Table 1 presents the basic crystallographic data of polymorphic modifications of LiAlO_2 .

The tetragonal $\gamma\text{-LiAlO}_2$ is considered to be the most thermodynamically stable polymorphic modification of LiAlO_2 and it is considered to be a potential material for obtaining tritium for the purposes of nuclear fusion, substrates for epitaxial growth of II-V semiconductors such as GaN, components for the production of liquid carbonate fuel cells or radiation dosimeters^{9,12,15–17,37–39}. In recent years, however, attention has been paid to the hexagonal form of $\alpha\text{-LiAlO}_2$ ^{38–44}. It has been shown that at the operating temperature of the fuel cell equal to 650 °C, the alpha variety is more stable than the gamma variety⁴¹. The $\alpha\text{-LiAlO}_2$ polymorph is also considered as a component for the production of electrode protective layers in lithium batteries^{40–42}. A necessary condition for the use of $\alpha\text{-LiAlO}_2$, however, is to obtain a product containing nanometric grain size.

The literature review shows that the $\alpha\text{-LiAlO}_2$ formed at temperatures not exceeding 600 °C is nanocrystalline, however, it is most often contaminated with substrates or by-products of the synthesis reaction^{45,46}. The large broadening of the diffraction reflections of the $\alpha\text{-LiAlO}_2$ obtained in such conditions is related to the presence of crystallites with dimensions of the order of 7–15 nm and a strong structure defect. SEM and TEM microscopic studies revealed the presence of dislocations and inclusions of spinel-like fragments or amorphous areas in the $\alpha\text{-LiAlO}_2$ samples tested⁶. On the other hand, at temperatures above 650 °C, a slowly progressing phase transition under these conditions begins, leading to the tetragonal $\gamma\text{-LiAlO}_2$ ^{27,40}.

The conducted literature review showed that the authors of the studies disagreed as to the temperature of phase transitions and the thermal stability of the LiAlO_2 polymorphs. Lejus^{20,47}, found that at 900 °C, $\alpha\text{-LiAlO}_2$ undergoes a reversible transformation to the high-temperature γ polymorph however, the transformation from γ to α is very slow. LiAlO_2 melts at 1700 °C, but at temperatures higher than 1300 °C, it decomposes into LiAl_5O_8 and Li_2O , caused by the high volatility of lithium oxide. According to Lehmann et al.²⁷ slow irreversible

transformation of $\alpha \rightarrow \gamma$ -LiAlO₂ occurs at temperatures above 600 °C. Hummel and co-workers⁴⁸ claim that the α phase undergoes a rapid phase transition at the temperature of 1200–1300 °C, and the melting point of LiAlO₂ is equal to 1610 ± 15 °C.

Isupov et al.⁴⁹ investigated the effect of the gaseous atmosphere on the type of LiAlO₂ modification produced using gibbsite and Li₂CO₃ mixture. They showed that during synthesis at 800 °C in air with typical partial water pressure of 1300 Pa forms α -LiAlO₂ contaminated with small amounts of γ -LiAlO₂. Synthesis in helium with water partial pressure not exceeding 4 Pa form both modifications in similar amounts but in vacuum with water pressure of 0.1 Pa mostly γ -LiAlO₂ is formed.

The structure of the α -LiAlO₂³⁰, β -LiAlO₂³¹, γ -LiAlO₂³³ and δ -LiAlO₂³⁴ is known. The crystal lattice of the hexagonal layered α -LiAlO₂ and the high-pressure tetragonal δ -LiAlO₂ are deformed variants of the NaCl structure with ordered Li⁺ and Al³⁺ ions in the octahedral sites. In the structure of γ -LiAlO₂³³ LiO₄ and AlO₄ tetrahedra connected by common corners form layers that connect to adjacent layers by common edges. In turn, the β -LiAlO₂ crystal lattice with a deformed wurtzite structure is built of LiO₄ and AlO₄ tetrahedrons connected via common corners³¹.

IR spectra of α -LiAlO₂, β -LiAlO₂ and γ -LiAlO₂ are known^{32, 47, 50–52}.

La Ginestra and co-workers⁵³, as a result of heating at 400 °C for 500 hours of the mixture of γ -Al₂O₃ and Li₂O₂ obtained the Li₃AlO₃ phase and presented the powder diffraction pattern of this compound. The authors did not manage to obtain single-phase Li₃AlO₃ sample, but only a mixture containing about 40% of unreacted reagents. According to the researchers, the Li₃AlO₃ is metastable and above 420 °C it decomposes with the release of α -LiAlO₂ and Li₅AlO₄⁵³. The authors of the study failed to obtain the Li₃AlO₃ phase with the use of Li₂CO₃, LiNO₃ and Li₂O⁵³. The existence of the Li₃AlO₃ compound was also postulated by Kroger and Fingars⁵⁴ and Fedorov and Shamari⁵⁵, but the compound was not characterized by them.

EXPERIMENTAL

The following materials were used for the research: Li₂CO₃, a.p. (POCh, Poland), LiOH·H₂O (Loba Chemie, Austria), Al₂O₃ pure, sintered, denoted as Al₂O₃-sl (POCh, Poland), boehmite- γ -AlOOH (POCH, Poland) and Al(NO₃)₃·9H₂O a.p. (POCH, Poland). α -Al₂O₃ was obtained by sintering Al₂O₃-sl at 1200 °C for 4 hours.

The syntheses of Li₃AlO₃ and LiAlO₂ were carried out using a conventional solid-state reaction method, analogous to that presented in^{56–59}.

The substrates weighed in suitable proportions were homogenized in an agate mortar and calcinated in the temperature range of 400–1200 °C in 24 h stages. The samples were heated in the furnace FCF 3.5/1350 (Czylok, Poland). Temperatures of calcination of samples were estimated basing on literature data concerning Li₂O-Al₂O₃ system^{19, 21, 23, 29, 47, 48, 55}.

In the frames of this work new method of LiAlO₂ synthesis was developed. Lithium carbonate and aluminum nitrate(V) nonahydrate weighed in stoichiometric proportions were ground in a mortar until the release of CO₂ bubbles ceases. The semi-finished product thus obtained was in the form of a paste. Subsequently, the paste obtained was heated in an air atmosphere in the temperature range of 400–600 °C, then, after taking it out of the furnace, it was cooled to room temperature in desiccator, ground in a mortar and subjected to X-ray investigations.

The phase composition of samples was investigated by using XRD method and identified by powder diffraction patterns of obtained samples recorded with the aid of the diffractometer EMPYREAN II, (PANalytical, The Netherlands) using the CuK α radiation with a graphite monochromator with the help of Highscore + software and PDF4+ICDD database. The powder diffraction patterns of selected phases were indexed using the REFINEMENT program of DHN/PDS package.

The IR spectra were recorded on the SPECORD M 80 spectrometer (Carl Zeiss, Jena, Germany). The measurements were made within the wavenumber range of 4000–200 cm⁻¹. The infrared spectra were made by pelleting a sample with KBr in the weight ratio of 1:300.

The mean crystallite size of selected samples was calculated using the Scherrer formula:

$$D_{hkl} = \frac{k \cdot \lambda}{\beta \cdot \cos \theta}$$

where: β – the half-width of the reflex (hkl) [rad],

D_{hkl} – mean crystallite size in the direction perpendicular to the plane (hkl) [Å],

λ – wavelength of the X-ray radiation used, $\lambda = 1.5406$ [Å],

k – Scherrer's constant equal to $k = 0.94$,

θ – reflection angle, related to the reflection (hkl) [°].

RESULTS AND DISCUSSION

Transition modifications of alumina such as γ -, η -, δ - and θ - Al₂O₃ obtained in the temperature range

Table 1. Basic crystallographic data of α -LiAlO₂, β -LiAlO₂, γ -LiAlO₂ and δ -LiAlO₂ phases, where CS-crystal system: O – orthorhombic, T – tetragonal, H – hexagonal HP (GPa)-modification obtain under high pressure equal to (GPa), SG (no.) – space group and its number; D – distorted structure, TW – this work

Formula	Li ₂ O [% mol]	Structure type	CS	SG (no.)	Unit cell parameters			Ref
					a [Å]	b [Å]	c [Å]	
α -LiAlO ₂	50.0	α -NaFeO ₂	H	R-3m (166)	2.7993	2.793	14.180	[29]
α -LiAlO ₂	50.0		H		2.8020	2.8020	14.2246	TW
β -LiAlO ₂	50.0	β -NaFeO ₂ D Wurtzite	O	Pna2 ₁ (33)	5.2800	6.300	4.900	[30]
β -LiAlO ₂	50.0		O		5.272	6.299	4.903	TW
γ -LiAlO ₂	50.0	γ -LiAlO ₂	T	P4 ₂ ,2 (90)	5.1687	5.1687	6.2679	[33]
γ -LiAlO ₂	50.0		T		5.1724	5.1724	6.2756	TW
δ -LiAlO ₂	50.0	D NaCl HP (9 GPa)	T	I4 ₁ /amd (141)	3.8866	3.8866	8.3001	[34]

400–1000 °C have a defective spinel structure based on a cubic close packed lattice of oxide ions^{60, 61}. For this reason, the powder diffraction patterns of individual modifications reported in the literature are similar to each other (similar d_{hkl} values). It is very difficult to clearly identify these transition alumina. In this work, when writing about this type of phases, we will use the common symbol $\text{Al}_2\text{O}_3\text{-sl}$ (spinel like).

In the first stage of investigations synthesis of LiAlO_2 was carried out using Li_2CO_3 and $\alpha\text{-Al}_2\text{O}_3$, $\text{Al}_2\text{O}_3\text{-sl}$ and boehmite as aluminum precursors. Figures 1A and 1B show fragments of powder diffractograms of the reaction mixtures prepared with the use of $\text{Al}_2\text{O}_3\text{-sl}$ and Li_2CO_3 (Fig. 1A) or of $\alpha\text{-Al}_2\text{O}_3$ and Li_2CO_3 (Fig. 1B) with the compositions corresponding to the LiAlO_2 phase, and samples recorded after successive heating stages in the temperature range of 450–1000 °C.

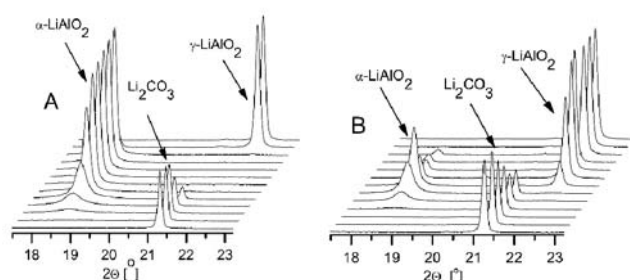


Figure 1. Fragments of the powder diffractograms of the reaction mixture prepared with the use of $\text{Al}_2\text{O}_3\text{-sl}$ and Li_2CO_3 (A) and with the use of $\alpha\text{-Al}_2\text{O}_3$ and Li_2CO_3 (B) with the composition corresponding to the LiAlO_2 phase and samples recorded after successive heating stages in the temperature range of 450–1000 °C

During the heating stage at 450 °C, almost all boehmite used in the synthesis decomposed to form $\text{Al}_2\text{O}_3\text{-sl}$, and the further synthesis process was carried out in this sample with the use of in situ formed precursor. A single-phase sample containing $\alpha\text{-LiAlO}_2$ was obtained using boehmite and $\text{Al}_2\text{O}_3\text{-sl}$ after the heating stage at the temperature of 700 °C. In both cases, the $\alpha\text{-LiAlO}_2$ modification appeared in reaction mixtures after a heating stage at 500 °C. Pure $\alpha\text{-LiAlO}_2$ obtained after sintering at 700 °C was stable up to the temperature of 900 °C, at which the slow phase change leading to $\gamma\text{-LiAlO}_2$ began. However, a single-phase sample of $\gamma\text{-LiAlO}_2$ was obtained only after the heating stage at 1000 °C. The reaction of LiAlO_2 synthesis with the use of corundum was much slower. During it, the $\alpha\text{-LiAlO}_2$ modification appeared in the reaction mixture after a heating stage at 550 °C, but we failed to obtain a single-phase sample of $\alpha\text{-LiAlO}_2$. On the other hand small amounts of $\gamma\text{-LiAlO}_2$ were detected after the heating stage at 650 °C while the pure $\gamma\text{-LiAlO}_2$ was obtained after the heating stage at 950 °C (Fig. 1A and 1B).

In the frames of this work new method of LiAlO_2 synthesis was developed using a mixture of aluminum nitrate(V) and lithium carbonate as reactants. Grinding of the Li_2CO_3 and $\text{Al}(\text{NO}_3)_3 \cdot 9\text{H}_2\text{O}$ solids initiates the reaction between them, as evidenced by CO_2 gas bubbles intensively emitted during the grinding of the reagents in the mortar. The reaction is probably favored

by a very large number of crystallization water molecules contained in the crystal lattice of aluminum nitrate(V) nanohydrate, which, released during intense grinding, enables the aluminum nitrate(V) hydrolysis reaction leading to strong acidification of the reaction medium and initiates the decomposition of Li_2CO_3 . The mechanism of this process is currently being researched and the results will be presented in the next paper. The paste obtained after the evolution of CO_2 bubbles had ceased was then heated in a furnace under an air atmosphere in the temperature range of 400–600 °C. Figure 2 shows the diffractograms recorded after the successive stages of heating the obtained paste.

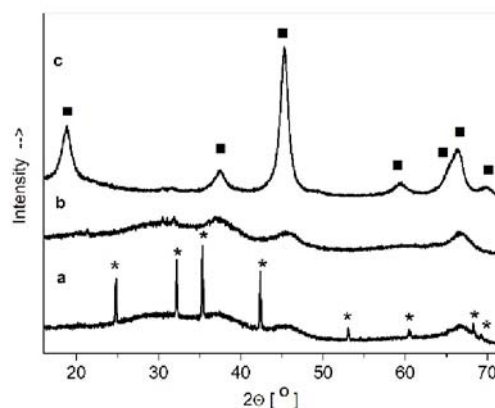


Figure 2. Powder diffraction patterns recorded during the synthesis of $\alpha\text{-LiAlO}_2$ with a new method using Li_2CO_3 and $\text{Al}(\text{NO}_3)_3 \cdot 9\text{H}_2\text{O}$ after the heating steps at the following temperatures: a – 400 °C x 30 min, b – 400 °C x 30 min, c – 600 °C x 30 min. * – means LiNO_3 , ■ – means $\alpha\text{-LiAlO}_2$

Single-phase sample containing $\alpha\text{-LiAlO}_2$ was obtained after 30 minutes of heating at 600 °C, while the synthesis with $\text{Al}_2\text{O}_3\text{-sl}$ and Li_2CO_3 required heating the reactants at 700 °C. Lithium nitrate(V) melts at 255 °C, and boils and decomposes at 600 °C. The presence of LiNO_3 reflections (PDF 04-010-5519) on the diffractogram of the reaction mixture after the heating step at 400 °C for 30 minutes shows that even molten LiNO_3 slowly reacts with the components of the reaction mixture. The $\alpha\text{-LiAlO}_2$ obtained at the temperature of 600 °C x 30 min was characterized by strongly broadened diffraction reflections, and the average size of crystallites in this preparation determined by the Scherrer method was equal to 75 Å. This value is consistent with the results of the research presented in⁶, where the effect of calcination time of the $\alpha\text{-LiAlO}_2$ sample at 600 °C on the size of crystallites was analyzed. The reason for the significant broadening of diffraction reflections is, inter alia, a high concentration of defects in the crystal lattice of $\alpha\text{-LiAlO}_2$ obtained at low temperatures⁶. It should be mentioned, however, that regardless of the type of metal precursors used in the synthesis of $\alpha\text{-LiAlO}_2$, the reflexes of this phase were considerably broadened. The crystallite size determined by the Scherrer method during the synthesis of $\alpha\text{-LiAlO}_2$ with the use of Li_2CO_3 and boehmite increased gradually with the increase of temperature from 101 Å (600 °C x 24 h) through 389 Å (700 °C x 24 h) to 406 Å (850 °C x 24 h).

The literature review showed that the Li_3AlO_3 phase obtained by La Ginestra et al.⁵³ is relatively poorly

studied. Taking into account the comments of the authors of the work⁵³, an attempt was made to obtain the Li_3AlO_3 phase by heating a mixture of $\text{LiOH}\cdot\text{H}_2\text{O}$ and $\text{Al}_2\text{O}_3\text{-sl}$ with a composition corresponding to the Li_3AlO_3 phase in the temperature range of 400–500 °C. The diffractograms recorded after the first and second heating steps at 400 °C for 72 h resembled that of the Li_3AlO_3 phase presented by Ginestera. However, X-ray phase analysis showed that the samples obtained at 400 °C were not single-phase and contained a mixture of LiOH (PDF 00-032-0564), Li_2CO_3 and $\beta\text{-LiAlO}_2$ (PDF 00-033-0785) (Fig. 3).

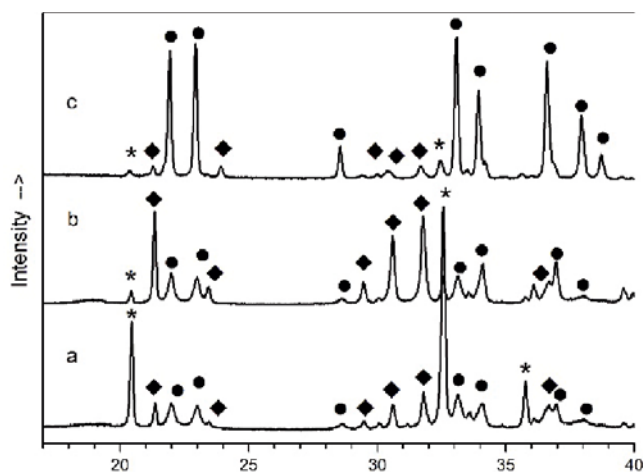


Figure 3. Fragments of the powder diffraction patterns recorded after successive stages of heating the mixture of $\text{LiOH}\cdot\text{H}_2\text{O}$ and $\text{Al}_2\text{O}_3\text{-sl}$ with the composition corresponding to the formula Li_3AlO_3 : a – 1st stage 400 °C x 72 h, b – 2nd stage 400 °C x 72 h and c – 3rd stage-500 °C x 72 h, where * – LiOH , ● – $\beta\text{-LiAlO}_2$ and ◆ – Li_2CO_3

However, individual reflections from the Li_3AlO_3 diffractogram presented by Ginestera were shifted by 0.01–0.20 degrees towards higher 2Theta angles in relation to the position on our diffractograms and data contained in PDF cards of LiOH , Li_2CO_3 and $\beta\text{-LiAlO}_2$. Therefore, the conducted research shows that the phase with the formula Li_3AlO_3 is not formed. According to the literature data, LiOH identified in reaction mixtures may be formed as a result of the reaction of Li_2O with water contained in the air. LiOH is also formed as a result of dehydration of $\text{LiOH}\cdot\text{H}_2\text{O}$ in the temperature range 90–200 °C and then in the temperature range 420–550 °C it decomposes with the release of Li_2O ⁴⁹. The presence of Li_2CO_3 in the obtained samples can also be explained because both $\text{LiOH}\cdot\text{H}_2\text{O}$ and LiOH have the ability to bind large amounts of CO_2 from the air to form Li_2CO_3 ⁴⁹. After another heating step at 500 °C for 72 h, the content of $\beta\text{-LiAlO}_2$ in the sample increased significantly. This fact prompted us to try to synthesize $\beta\text{-LiAlO}_2$ using a stoichiometric mixture of $\text{LiOH}\cdot\text{H}_2\text{O}$ and $\text{Al}_2\text{O}_3\text{-sl}$. Figure 4 shows the diffractograms of the sample with the composition LiAlO_2 after subsequent stages of heating. The analysis of the XRD test results showed that the reaction mixture after the first stage of heating at 500 °C for 72 h contained $\beta\text{-LiAlO}_2$ as the main component, accompanied by Li_2CO_3 and $\alpha\text{-LiAlO}_2$ in much smaller amounts. After the second stage of heating at 650 °C for 24 hours, the obtained product

contained a mixture of α - and $\beta\text{-LiAlO}_2$, and the intensity of reflections characteristic of $\alpha\text{-LiAlO}_2$ increased. The sample after the heating step at 700 °C for 24 h contained $\gamma\text{-LiAlO}_2$ as the main component, accompanied by lower amounts of α - and $\beta\text{-LiAlO}_2$.

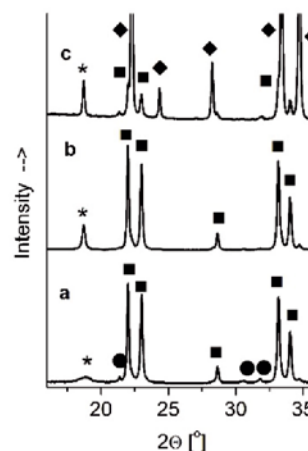


Figure 4. Fragments of the powder diffraction patterns recorded after successive stages of heating the mixture of $\text{LiOH}\cdot\text{H}_2\text{O}$ and $\text{Al}_2\text{O}_3\text{-sl}$ with the composition corresponding to the formula LiAlO_2 : a – 1st stage 500 °C x 72 h, b – 2nd stage 650 °C x 72 h and c – 3rd stage-700 °C x 72 h, where * – $\alpha\text{-LiAlO}_2$, ■ – $\beta\text{-LiAlO}_2$, ◆ – $\gamma\text{-LiAlO}_2$ and ● – Li_2CO_3

The conducted research indicates that the use of $\text{LiOH}\cdot\text{H}_2\text{O}$ as a lithium precursor promotes the formation of $\beta\text{-LiAlO}_2$. However, while striving to eliminate lithium carbonate from the reaction mixture by increasing the reaction temperature, the content of the $\alpha\text{-LiAlO}_2$ is simultaneously increased, and above 650 °C $\beta\text{-LiAlO}_2$ undergoes a phase transition to $\gamma\text{-LiAlO}_2$. Currently, research is conducted to obtain a single-phase $\beta\text{-LiAlO}_2$ sample and the results will be published soon.

The powder diffractograms of the $\beta\text{-LiAlO}_2$, $\gamma\text{-LiAlO}_2$ and $\alpha\text{-LiAlO}_2$ phases were indexed using the Refinement program. The calculated values of the unit cell parameters are shown in Table 1. In the case of $\beta\text{-LiAlO}_2$, the results of the powder diffractogram pattern indexing are presented in Table 2.

Table 2. The result of the indexing of X-ray powder diffraction pattern of $\beta\text{-LiAlO}_2$ obtained in this work

Lp.	d_{exp} [nm]	d_{cal} [nm]	(hkl)	I/I_0 [%]
1.	4.0479	4.0431	110	98
2.	3.8737	3.8693	011	86
3.	3.1218	3.1194	111	16
4.	2.7050	2.7039	120	100
5.	2.6377	2.6362	200	55
6.	2.4532	2.4516	002	59
7.	2.3690	2.3678	121	25
8.	2.3237	2.3219	201	10
9.	2.1787	2.1786	211	4
10.	2.0967	2.0963	112	6
11.	1.9299	1.9302	031	3
12.	1.8149	1.8126	131	22
13.	1.7958	1.7953	202	9
14.	1.7270	1.7265	212	2
15.	1.6419	1.6424	230	1
16.	1.5997	1.6001	311	4
17.	1.5745	1.5748	040	5
18.	1.5343	1.5347	320	34
19.	1.3980	1.3987	123	16
20.	1.3892	1.3891	203	6

To know better properties of obtained phases IR spectra of γ -LiAlO₂, β -LiAlO₂ and α -LiAlO₂ were recorded. Analysis of the number and positions of absorption bands recorded in their IR spectra has shown good agreement with literature data^{32, 47, 50-52}.

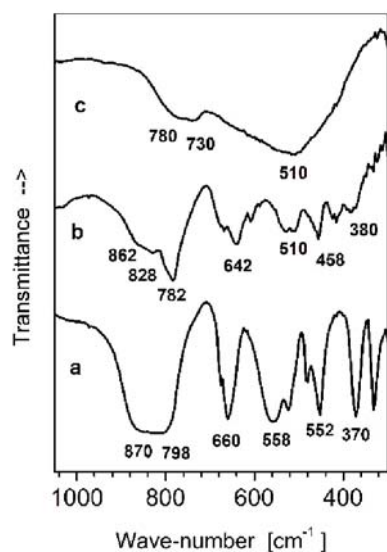


Figure 5. IR spectra of: a) γ -LiAlO₂, b) β -LiAlO₂, c) α -LiAlO₂

Figure 5 shows the IR spectra of γ -LiAlO₂ (curve a), β -LiAlO₂ (curve b) and α -LiAlO₂ (curve c). The literature survey has shown that crystal lattices of γ -LiAlO₂ and β -LiAlO₂ are built up of LiO₄ and AlO₄ tetrahedra, when α -LiAlO₂ of LiO₆ and AlO₆ octahedra^{32, 47, 50-52}. The presence of LiO₄ and AlO₄ tetrahedra in crystal lattices of γ -LiAlO₂ (Fig. 5, curve a) and β -LiAlO₂ (Fig. 5, curve b) with Li-O and Al-O bonds shorter than in the case of LiO₆ and AlO₆ octahedra is responsible for the shift of absorption bands in their spectra towards higher wavenumbers in comparison with the position of IR bands in the spectrum of α -LiAlO₂. Moreover, good agreement of the number and positions of absorption bands in IR spectrum of β -LiAlO₂ obtained in our laboratory with data in paper³⁵ corroborates that polymorph of LiAlO₂ obtained by Chang crystallizes in an orthorhombic system.

CONCLUSIONS

Using applied procedures of syntheses, three phases have been obtained: α -LiAlO₂, β -LiAlO₂, γ -LiAlO₂.

A new method of LiAlO₂ synthesis was developed consisting in grinding in mortar mixture of lithium carbonate and aluminum nitrate(V) nonahydrate until the release of CO₂ bubbles ceases and subsequent heating of obtained paste in the temperature range of 400–600 °C.

As a result of the reaction of LiOH H₂O with Al₂O₃-sl, β -LiAlO₂ was obtained, contaminated with a small amount of α -LiAlO₂.

It has been shown that the powder diffractogram of the Li₃AlO₃ phase is a set of diffraction reflections that can be attributed to the mixture of LiOH, Li₂CO₃ and β -LiAlO₂.

The results of XRD and IR investigations showed that β -LiAlO₂ crystallizes in an orthorhombic system.

LITERATURE CITED

1. Rebouças, L.B., Souza, M.T., Raupp-Pereira, F., & Novaes de Oliveira, A.P. (2019). Characterization of Li₂O-Al₂O₃-SiO₂ glass-ceramics produced from a Brazilian spodumene concentrate. *Cerâmica* 65, 366–377. DOI: 10.1590/0366-69132019653752699.
2. Ahmadi, Moghadam, H. & Hossein, Paydar, M. (2016). The Effect of Nano CuO as Sintering Aid on Phase Formation, Microstructure and Properties of Li₂O-Stabilized β '-Alumina Ceramics. *J. Ceram. Sci. Tech.*, 07(04), 441–446. DOI: 10.4416/JCST2016-00075.
3. Shackelford, J.F. & Doremus, R.H. (2008). Ceramic and glass materials. Structure, properties and processing. Springer Science+Business Media LLC New York. ISBN 978-0-387-73361-6.
4. Dhabeekar, B., Raja, E.A., Gundu Rao, T.K., Kher, R.K. & Bhat, B.C. (2009). Thermoluminescence, optically stimulated luminescence and ESR studies on LiAl₃O₈:Tb. *Indian. J. Pure Ap. Phy.*, 47, 426–428.
5. Mandowska, E., Mandowski, A., Bilski, P., Marczevska, B., Twardak, A. & Gieszczyk, W. (2015). Lithium aluminate – a new detector for dosimetry. *Prz. Elektrotech.* 91(9), 117–120 (in Polish).
6. Gao, J., Shi, S., Xiao, R. & Li, H. (2016). Synthesis and ionic transport mechanisms of α -LiAlO₂. *Solid State Ionics*, 286, 122–134. DOI: 10.1016/j.ssi.2015.12.028.
7. Özkan, G. & Incirkuş Ergençoglu, V. (2016). Synthesis and characterization of solid electrolyte structure material (LiAlO₂) using different kinds of lithium and aluminum compounds for molten carbonate fuel cells. *Indian J. Chem. Technol.* 23, 227–231.
8. Kim, J.E., Patil, K.Y., Han, J., Yoon, S.P., Nam, S.W., Lim, T.H., Hong, S.A., Kim, H. & Lim, H.Ch. (2009). Using aluminum and Li₂CO₃ particles to reinforce the α -LiAlO₂ matrix for molten carbonate fuel cells. *Internat. J. Hydrogen Energy* 34(22), 9227–9232. DOI: 10.1016/j.ijhydene.2009.08.069.
9. Ducan, Y. (2021). Theoretical Investigation of the CO₂ Capture Properties of γ -LiAlO₂ and α -Li₅AlO₄. *Micro Nanosyst.* 13, 32–41. DOI: 10.2174/1876402911666190913184300.
10. Ávalos-Rendón, T., Casa-Madrid, J. & Pfeiffer, H. (2009). Thermochemical Capture of Carbon Dioxide on Lithium Aluminates (LiAlO₂ and Li₅AlO₄): A New Option for the CO₂ Absorption. *J. Phys. Chem. A*, 113, 6919–6923. DOI: 10.1021/jp902501v.
11. Raja, M., Sanjeev, G., Kumar, T.P. & Stephan, A.M. (2015). Lithium aluminate-based ceramic membranes as separators for lithium-ion batteries. *Ceram. Int.* 41, 3045–50. DOI: 10.1016/j.ceramint.2014.10.142.
12. Fouad, O.A., Farghaly, F.I. & Bahgat, M. (2007). A novel approach for synthesis of nanocrystalline γ -LiAlO₂ from spent lithium-ion batteries. *J. Anal. Appl. Pyrolysis.* 78, 65–69. DOI: 10.1016/j.jaap.2006.04.002.
13. Pollard, V.A., Young, A., McLellan, R., Kennedy, A.R., Tuttle, T., Robert, E. & Mulvey, R.E. (2019). Lithium-Aluminate-Catalyzed Hydrophosphination Applications. *Angew. Chem. Int. Ed.* 58, 1229–12296. DOI: 10.1002/anie.201906807.
14. Indris, S. & Heitjans, P. (2006). Local electronic structure in a LiAlO₂ single crystal studied with ⁷Li NMR spectroscopy and comparison with quantum chemical calculations. *Phys. Rev. B* 74, 245120-1-5. DOI: 10.1103/PhysRevB.74.245120.
15. Duan, Y., Sorescu, D.C., Jiang, W. & Senor, D.J. (2020). Theoretical study of the electronic, thermodynamic, and thermo-conductive properties of γ -LiAlO₂ with ⁶Li isotope substitutions for tritium production. *J. Nucl. Mater.* 530, 151963. DOI: 10.1016/j.nuclmat.2019.151963.
16. Rasneur, B. (1985). Tritium breeding material γ -LiAlO₂. *Fusion Technol.* 8, 1909–1914. DOI: 10.13182/FST85-A40040.

17. Liu, Y.Y., Billone, M.C., Fischer, A.K., Tam, S.W., Clemmer, R.G. & Hollenberg, G.W. (1985). Solid tritium breeder materials Li_2O and LiAlO_2 - a data-base review. *Fusion Sci. Technol.* 8, 1970–1984. DOI: 10.13182/FST85-A24573.
18. Morley, N.B., Abdou, M.A., Anderson, M., Calderoni, P., Kurtz, R.J., Nygren, R., Raffray, R., Sawan, M., Sharpe, P., Smolentsev, S., Willms, S. & Ying, A.Y. (2006). Overview of fusion nuclear technology in the US. *Fusion Eng. Des.* 81, 33–43. DOI: 10.1016/j.fusengdes.2005.06.359.
19. Strickler, D.W. & Roy, R. (1961). Studies in the System $\text{Li}_2\text{O}-\text{Al}_2\text{O}_3-\text{Fe}_2\text{O}_3-\text{H}_2\text{O}$. *J. Am. Ceram. Soc.* 44, 5, 225–230. DOI: 10.1111/j.1151-2916.1961.tb15365.x.
20. Lejus, A.M. & R. Collongues, R. (1962). Sur la structure les propriétés des aluminates de lithium. *Chimie Minérale* 2005–2007.
21. Kriens, M., Adiwidjaja, G., Guse, W., Klaska, K.H., Lathe, C. & Saalfeld, H. (1996). The crystal structures of LiAl_5O_8 and $\text{Li}_2\text{Al}_4\text{O}_7$. *N. Jb. Miner. Mh.* 8, 344–350.
22. Hatch, R.A. (1943). Phase equilibrium in the system: $\text{Li}_2\text{O}-\text{Al}_2\text{O}_3-\text{SiO}_2$. *Am. Mineral.* 28, 471–496. DOI: 10.1111/j.1151-2916.1985.tb15280.x.
23. Cook, L.P. & Plante, E.R. (1992). Phase Diagram of the System $\text{Li}_2\text{O}-\text{Al}_2\text{O}_3$. *Ceram. Trans.* 27, 193–222.
24. Byker, H.J., Eliezer, I., Eliezer, N. & Howald, R.A. (1979). Calculation of a Phase Diagram for $\text{LiO}_{0.5}-\text{AlO}_{1.5}$ System. *J. Phys. Chem.* 83, 18, 2349–2355. DOI: 10.1021/j100481a009.
25. Konar, B., Van Ende, M.A. & Junh, I.H. (2018). Critical Evaluation and Thermodynamic Optimization of the $\text{Li}_2\text{O}-\text{Al}_2\text{O}_3$ and $\text{Li}_2\text{O}-\text{MgO}-\text{Al}_2\text{O}_3$ Systems. *Metall. Mat. Trans. B* 49, 2917–2944. DOI: 10.1007/s11663-018-1349-x.
26. Marezio, M. & Remeika, J.P. (1966). High-pressure synthesis and crystal structure of $\alpha\text{-LiAlO}_2$. *J. Chem. Phys.* 44, 3143–4. DOI: 10.1063/1.1727203.
27. Lehmann, H.A. & Hesselbrarh, H.Z. (1961). Über eine neue Modifikation des LiAlO_2 . *Anorg. Allg. Chem.* 313, 117–120. DOI: 10.1002/zaac.19613130110.
28. Dronskowski, R. (1993). Reactivity and acidity of Li in LiAlO_2 phases. *Inorg. Chem.* 32, 1–9. DOI: 10.1021/ic00053a001.
29. Poeplmeyer, K.R., Chiang, C.K. & Kipp, D.O. (1988). Synthesis of High-Surface-Area $\alpha\text{-LiAlO}_2$. *Inorg. Chem.* 27, 4523–4524. DOI: 10.1021/ic00298a002.
30. Thery, J. (1961). Structure and properties of alkaline aluminates. *Bull. Soc. Chim. Fr.* 973–5.
31. Marezio, M. (1965). The Crystal Structure of LiGaO_2 . *Acta Cryst.* 18, 481–484. DOI: 10.1107/S0365110X65001068.
32. Marezio, M. (1965). The Crystal Structure and Anomalous Dispersion of $\gamma\text{-LiAlO}_2$. *Acta Cryst.* 19, 396–400. DOI: 10.1107/S0365110X65003511.
33. Li, X., Kobayashi, T., Zhang, F., Kimoto, K. & Sekine, T. (2004). A new high-pressure phase of LiAlO_2 . *J. Solid State Chem.* 177, 1939–1943. DOI: 10.1016/j.jssc.2003.12.014.
34. Lei, L., He, D., Zou, Y. & Zhang, W. (2008). Phase transitions of LiAlO_2 at high pressure and high temperature. *J. Solid State Chem.* 181, 1810–1815. DOI: 10.1016/j.jssc.2008.04.006.
35. Chang, C.H. & Margrave, J.L. (1968). Highpressure-high temperature synthesis. III. Direct synthesis of new high-pressure forms of LiAlO_2 and LiGaO_2 and polymorphism in LiMO_2 compounds ($M=\text{B}, \text{Al}, \text{Ga}$). *J. Amer. Chem. Soc.* 90, 2020–2022. DOI: 10.1021/ja01010a018.
36. Debray, L. & Hardy, A.C.R. (1960). Contribution a l'étude structurale des aluminates de lithium. *Hebd. Seances Acad. Sci.* 251, 725–726.
37. Waltereit, P., Brandt, O., Trampert, A., Grahn, H.T., Meninger, J., Ramsteiner, M., Reiche, M. & Ploog, K.H. (2000). Nitride semiconductors free of electrostatic fields for efficient white light-emitting diodes. *Nature* 406, 865–868. DOI: 10.1038/35022529.
38. Wiedemann, D., Indris, S., Meyen, M. & Pedersen, B. (2016) Single-crystal neutron diffraction on $\gamma\text{-LiAlO}_2$: Structure determination and estimation of lithium diffusion pathway. *Zeitschrift für Kristallographie – Crystalline Materials.* 231(3), 189–193. DOI: 10.14279/depositonce-5480.
39. Ha, N.T.T., Van Giap, T. & Thanh, N.T. (2020). Synthesis of lithium aluminate for application in radiation dosimetry. *Mater. Lett.* 267, 127506. DOI: 10.1016/j.matlet.2020.127506.
40. Jimenez-Becerril, J. & Garcia-Sosa, I. (2011). Synthesis of lithium aluminate by thermal decomposition of a lithium dawsonite-type precursor. *J. Ceram. Process. Res.* 12, 52–56.
41. Heo, S.J., Batra, R., Ramprasad, R. & Singh, P. (2018). Crystal morphology and phase transformation of LiAlO_2 : combined experimental and first-principles Studies. *J. Phys. Chem. C* 222, 28797–28804. DOI: 10.1021/acs.jpcc.8b09716.
42. Patil, K.Y., Yoon, S.P., Han, J., Lim, T.H., Nam, S.W. & Oh, I.H. (2011). The effect of lithium addition on aluminum-reinforced $\alpha\text{-LiAlO}_2$ matrices for molten carbonate fuel cells. *Int. J. Hydrog. Energy*, 36, 6237–6247. DOI: 10.1016/j.ijhydene.2011.01.161.
43. Park, J.S., Meng, X., Elam, J.W., Hao, S., Wolverton, Ch., Kim, Ch. & Cabana, J. (2014). Ultrathin Lithium-Ion Conducting Coatings for Increased Interfacial Stability in High Voltage Lithium-Ion Batteries. *Chem. Mater.* 26, 3128–3134. DOI: 10.1021/cm500512n.
44. Cheng, F., Xin, Y., Huang, Y., Chen, J., Zhou, H. & Zhang, X. (2013). Enhanced electrochemical performances of 5 V spinel $\text{LiMn}_{1.58}\text{Ni}_{0.42}\text{O}_4$ cathode materials by coating with LiAlO_2 . *J. Power Sources.* 239, 181–188. DOI: 10.1016/j.jpowsour.2013.03.143.
45. Cao, H., Xia, B., Zhang, Y., Xu, N. (2005). LiAlO_2 -coated LiCoO_2 as cathode material for lithium ion batteries. *Solid State Ionics.* 176, 911–914. DOI: 10.1016/j.ssi.2004.12.001.
46. Danek, V., Tarniowy, M. & Suski, L. (2004) Kinetics of the $\alpha \rightarrow \gamma$ phase transformation in LiAlO_2 under various atmospheres within the 1073–1173 K temperatures range. *J. Mater. Sci.* 39, 2429–2435. DOI: 10.1023/B:JM SC.0000020006.46296.04.
47. Lejus, A.M. (1964). Sur la formation a haute temperature de spinelles non stoechiométriques et de phases dérivées dans plusieurs systèmes d'oxydes a base d'alumina et dans le système alumina-nitride d'aluminium. *Rev. Hautes Tempér. et Réfract.*, 1, 53–95.
48. Hummel, F.A., Sastry, B.S.R. & Wotring, D. (1958). Studies in Lithium Oxide Systems: II, $\text{Li}_2\text{O}-\text{Al}_2\text{O}_3-\text{Al}_2\text{O}_3$. *J. Am. Ceram. Soc.* 41, 3, 88–92. DOI: 10.1111/j.1151-916.1958.tb15448.x.
49. Isupov, V.P., Bulina, N.V. & Borodulina, I.A. (2017). Effect of Water Vapor Pressure on the Phase Composition of Lithium Monoaluminates Formed in the Interaction of Aluminum Hydroxide and Lithium Carbonate. *Zhurnal Prikladnoi Khimii*, 90, 986–991. DOI: 10.1134/S1070427217080043.
50. Tarte, P. (1967). Infra-red spectra of inorganic aluminates and characteristic vibrational frequencies of AlO_4 tetrahedra and AlO_6 octahedra. *Spectrochim. Acta* 23A, 2127–2143. DOI: 10.1016/0584-8539(67)80100-4.
51. Braun, P.A. (1952). Superstructure in Spinel. *Nature* 170, 1123. DOI: 10.1038/1701123a0.
52. Datta, R.K. & Roy, R. (1963). Phase Transitions in LiAl_5O_8 . *J. Am. Ceram. Soc.* 46, 8, 388–390. DOI: 10.1111/j.1151-2916.1963.tb11757.x.
53. La Ginestra, A., Lo Jacono, M. & Porta, P. (1972). The preparation, characterization, and thermal behaviour of some lithium aluminum oxides: Li_3AlO_3 and Li_5AlO_4 . *J. Thermal Anal.* 4, 5–17. DOI: 10.1007/bf02100945.
54. Kroger, C. & Fingas, E. (1935). Über die Systeme $\text{Alkalioxyd}-\text{CaO}-\text{Al}_2\text{O}_3-\text{SiO}_2-\text{CO}_2$. IV. Die CO_2 -Drucke des kieselsäurereichen Teils des Systems $\text{Li}_2\text{O}-\text{SiO}_2-\text{CO}_2$ und der Einwirkung von Al_2O_3 auf Li_2CO_3 . *Z anorg. Allg. Chem.* 224, 289–304. DOI: 10.1002/zaac.19352240309.
55. Fedorov, T.F. & Shamari, F.I. (1960). *Prim. Vak. V. Met., Akad. Nauk SSSR, Inst. Met. A.A. Baikova*, 137–142.

56. Walczak, J., Kurzawa, M. & Tabero, P. (1987). $V_9Mo_6O_{40}$ and phase equilibria in the system $V_9Mo_6O_{40}-Fe_2O_3$. *Thermochim. Acta* 118, 1–7. DOI: 10.1016/0040-6031(87)80065-5.
57. Tabero, P. (2010). Formation and properties of the new $Al_8V_{10}W_{16}O_{85}$ and $Fe_{8-x}Al_xV_{10}W_{16}O_{85}$ phases with the $M-Nb_2O_5$ structure. *J. Therm. Anal. Calorim.* 101, 560–566. DOI: 10.1007/s10973-010-0848-z.
58. Tabero, P., Frackowiak, A., Filipek, E., Dąbrowska, G., Homonnay, Z. & Szilágyi, P.Á. (2018). Synthesis, thermal stability and unknown properties of $Fe_{1-x}Al_xVO_4$ solid solution. *Ceram. Int.* 44, 17759–17766. DOI: 10.1016/j.ceramint.2018.06.243.
59. Filipek, E., Dąbrowska, G. & Piz, M. (2010). Synthesis and characterization of new compound in the V-Fe-Sb-O system. *J. Alloys Compd.* 490, 93–97. DOI: 10.1016/j.jallcom.2009.10.123.
60. Levin, I. & Brandon, D. (1998). Metastable Alumina Polymorphs: Crystal Structures and Transition Sequences. *J. Am. Ceram. Soc.* 81, 1995–2012. DOI: 10.1111/j.1151-2916.1998.tb02581.x.
61. Krokodis, X., Raybaud, P., Gobichon, A.E., Rebours, B., Euzen, P. & Toulhoat, H. (2001). Theoretical Study of the Dehydration Process of Boehmite to γ -Alumina. *J. Phys. Chem. B* 105, 5121–5130. DOI: 10.1021/jp0038310.
62. Kim, J., Kang, H., Hwang, K. & Yoon, S. (2019). Thermal Decomposition Study on Li_2O_2 for Li_2NiO_2 Synthesis as a Sacrificing Positive Additive of Lithium-Ion Batteries. *Molecules* 24, 4624–4632. DOI: 10.3390/molecules24244624.
63. Tovar, T.M. & Le, Van, M.D. (2017). Supported lithium hydroxide for carbon dioxide adsorption in water-saturated environments. *Adsorption* 23, 51–56. DOI: 10.1007/s10450-016-9817-6.